RAPID COMMUNICATIONS

PHYSICAL REVIEW B VOLUME 50, NUMBER 19 15 NOVEMBER 1994-I

Magnetic energy bands of carbon nanotubes

R. Saito
Department of Electronics Engineering, University of Electro-Communications, Chofugaoka, Chofu, 182 Tokyo, Japan

G. Dresselhaus
Francis Bitter National Magnet Laboratory, Massachusetts Institute of Technology, Cambridge, Massachusetts 02139

M. S. Dresselhaus
Department of Electrical Engineering and Computer Science and Department of Physics, Massachusetts Institute of Technology, Cambridge, Massachusetts 02139

(Received 11 August 1994; revised manuscript received 21 September 1994)

Landau quantization of the π energy bands of a carbon nanotube is calculated within the tight-binding approximation. The energy bands do not show explicit Landau levels, but they do have energy dispersion for all values of magnetic field. The energy bandwidth shows oscillations with a period that is scaled by a cross section of the unit cell of the tubule, which is specified by the symmetry of the nanotube.

Carbon nanotubes are of exceptional interest as one-dimensional (1D) materials on a nanometer length scale.[1] The electronic structure is especially significant in the sense that carbon nanotubes can be either metallic or semiconducting, depending only on the symmetry of the tube specified by a vector (see chiral vector, $\vec{C}_h$, in Fig. 1).[2–7] The magnetic response of the electronic structure for such one-dimensional materials with a two-dimensional surface is especially interesting, and is relevant to recent magnetoresistance[8] and susceptibility[9,10] experiments.

In a two-dimensional cosine band with lattice constant a, there is fractal behavior in the energy band spectra in a magnetic field H, depending on whether Ha^2/ϕ_0 is a rational or irrational number, where $\phi_0=hc/e$ is a flux quantum.[11] All energy dispersion relations are a periodic function of integer values of Ha^2/ϕ_0. However, the corresponding field is too large ($\sim 10^5$ T) to observe this fractal behavior explicitly. In relatively weak fields ($\sim 10^2$ T), we only observe Landau levels, except for Landau subbands near $E=0$ in the case of a 2D cosine band, since the wave functions near $E=0$ are for extended orbits.[12]

Ajiki and Ando[13] have shown an Aharanov-Bohm effect in carbon nanotubes for $H \parallel$ the tubule axis, and Landau level quantization for $H \perp$ the tubule axis. However, there is a limitation for using $\vec{k}\cdot\vec{p}$ perturbation theory around the degenerate point K at the corner of the hexagonal Brillouin zone in the case of a carbon nanotube, since the k values taken in the direction of the tubule circumference can be far from the K point, leading to incorrect values of the energy, especially for small carbon nanotubes and for energies far from that at the K point.

Here we present the magnetic energy band structure for carbon nanotubes within the tight-binding approximation, in which we use only the approximation that the atomic wave function is localized at a carbon site, and the magnetic field varies sufficiently slowly over a length scale equal to the lattice constant. This condition is valid for any large magnetic field, even if we adopt the smallest diameter carbon nanotube observed experimentally, whose diameter is 5 times as large as $a_{C\text{-}C}=1.421$ Å, the nearest-neighbor C-C distance.[2]

When the magnetic field H is applied perpendicular to the tubule axis, we can consider the two-dimensional vector potential $\mathbf{A}$ for the tubule surface as

$$\mathbf{A}=(0,(LH/2\pi)\sin(2\pi/L)x), \tag{1}$$

where L is the length of the chiral vector, $\vec{C}_h$, $(L=|\vec{C}_h|)$, and the coordinates x and y are taken along the circumferential and tubule axis directions, respectively (see Fig. 1).

For a chiral vector $\vec{C}_h=n\mathbf{a}_1+n\mathbf{a}_2=(n,m)$ (n,m are integers; $\mathbf{a}_1,\mathbf{a}_2$ are unit vectors), the unit cell of the tubule is a rectangle specified by $\vec{C}_h$ and a translational vector $\vec{T}$ as shown in Fig. 1,

$$\begin{aligned} &0<x<L, \quad L=a\sqrt{n^2+m^2+nm}, \\ &0<y<T, \quad T=|\vec{T}|=\sqrt{3}L/d_R\ , \end{aligned} \tag{2}$$

where a is the lattice constant of the honeycomb lattice ($a=\sqrt{3}a_{C\text{-}C}$), and the integer d_R being defined by the greatest common denominator d of the two integers n and m,[14,15] as

$$d_R=\begin{cases} 3d & \text{if } n-m \text{ is a multiple of } 3d \\ d & \text{if } n-m \text{ is not a multiple of } 3d. \end{cases} \tag{3}$$

When we use the vector potential, the wave vector k_y in the y direction remains a quantum number of translation even in the presence of a magnetic field ($-\pi<k_yT\leq\pi$). The wave vectors k_x in the x direction mix with each other in the presence of a magnetic field in accordance with Eq. (1). The number of the wave vectors in the x direction is N

$$k_x^r=(2\pi/L)(r/N) \quad (r=1,\ldots,N), \tag{4}$$

where N is the number of hexagons in the tubule unit cell given by[14,15]

$$N=2(n^2+m^2+nm)/d_R. \tag{5}$$

Since we have two inequivalent carbon sites A and B in the graphitic unit cell, we must solve a $2N\times 2N$ matrix to find the energy eigenvalues for a given k_y vector.

Within the tight-binding scheme, the Bloch functions for two equivalent carbon sites s ($s=A,B$) in a magnetic field can be expressed as

$$\Psi^s(\mathbf{k},\mathbf{r})=\frac{1}{\sqrt{N}}\sum_{\mathbf{R}}\exp\left(i\mathbf{k}\cdot\mathbf{R}+i\frac{e}{\hbar c}G_{\mathbf{R}}\right)\varphi_s(\mathbf{r}-\mathbf{R}), \quad (6)$$

where $G_{\mathbf{R}}$ is the phase factor associated with the magnetic field and is expressed by[16]

$$G_{\mathbf{R}}=\int_{\mathbf{R}}^{\mathbf{r}}\mathbf{A}(\boldsymbol{\xi})\cdot d\boldsymbol{\xi}=\int_0^1(\mathbf{r}-\mathbf{R})\cdot\mathbf{A}[\mathbf{R}+\lambda(\mathbf{r}-\mathbf{R})]d\lambda, \quad (7)$$

where the integration is taken on the line from $\mathbf{R}$ to $\mathbf{r}$. When the Hamiltonian in the magnetic field,

$$\mathscr{H}=(1/2m)[\mathbf{p}-(e/c)\mathbf{A}]^2+V, \quad (8)$$

operates on $\Psi^s(\mathbf{k},\mathbf{r})$, we obtain

$$\begin{aligned}\mathscr{H}\Psi^s(\mathbf{k},\mathbf{r})&=\frac{1}{\sqrt{N}}\sum_{\mathbf{R}}\exp(i\mathbf{k}\cdot\mathbf{R})\left[\frac{1}{2m}\left(\mathbf{p}-\frac{e}{c}\mathbf{A}\right)^2+V\right]\exp\left(i\frac{e}{\hbar c}G_{\mathbf{R}}\right)\varphi_s(\mathbf{r}-\mathbf{R})\\&=\frac{1}{\sqrt{N}}\sum_{\mathbf{R}}\exp\left(i\mathbf{k}\cdot\mathbf{R}+i\frac{e}{\hbar c}G_{\mathbf{R}}\right)\left[\frac{1}{2m}\left(\mathbf{p}-\frac{e}{c}(\mathbf{A}-\nabla G_{\mathbf{R}})\right)^2+V\right]\varphi_s(\mathbf{r}-\mathbf{R})\\&=\frac{1}{\sqrt{N}}\sum_{\mathbf{R}}\exp\left(i\mathbf{k}\cdot\mathbf{R}+i\frac{e}{\hbar c}G_{\mathbf{R}}\right)\left[\frac{\mathbf{p}^2}{2m}+V\right]\varphi_s(\mathbf{r}-\mathbf{R}). \quad (9)\end{aligned}$$

In obtaining the last line of Eq. (9), we use the fact that (1) the magnetic field is slowly changing compared with the change of $\varphi_s(\mathbf{r}-\mathbf{R})$, and (2) $\varphi_s(\mathbf{r}-\mathbf{R})$ is localized at $\mathbf{r}=\mathbf{R}$. Equation (9) is independent of the value of H and the functional form of $\mathbf{A}$.[16]

Using Eq. (9), we can calculate the matrix elements of $\mathscr{H}$ between two Bloch functions and solve the matrix to obtain the eigenvalues. It is noted here that we will have a term in $\exp[(ie/\hbar c)(G_{\mathbf{R}}-G_{\mathbf{R}'})]$ in the matrix elements, which is explicitly dependent on $\mathbf{r}$ as

$$G_{\mathbf{R}}-G_{\mathbf{R}'}=\int_{\mathbf{R}}^{\mathbf{R}'}\mathbf{A}(\boldsymbol{\xi})d\boldsymbol{\xi}+\Phi(\mathbf{r}), \quad (10)$$

where $\Phi(\mathbf{r})$ is the flux that penetrates the triangle defined by the three points, $\mathbf{R}$, $\mathbf{R}'$, and $\mathbf{r}$. However, we neglect this phase factor in the integrals over the atomic matrix element for simplicity. This approximation is valid when the magnetic field changes slowly compared with the lattice constant. This approximation is consistent with the assumption that we made above. The details of this formulation will be presented elsewhere.[17]

In Fig. 2, we show the energy dispersion curves E/γ_0 vs the dimensionless wave vector $\eta=k_yT/2\pi$ for a $\vec{C}_h=(10,0)$ nanotube at several values of the dimensionless inverse magnetic length $\nu=L/2\pi\ell$, where the magnetic length ℓ is defined by $\sqrt{c\hbar/eH}$, and ν has values: (a) 0.0, (b) 1.0, (c) 2.0, (d) 3.0 in Fig. 2. In the case of the 1D tubule $\vec{C}_h=(10,0)$, we have 40 ($=2N$) energy bands, some of which are twofold degenerate in the D_{10} point group.[4] There is no Landau level formation for the magnetic fields in Fig. 2. In two-dimensional graphite described by two-dimensional cosine bands, the magnetic field is constant over the two-dimensional plane, and thus the magnetic subbands have a small energy dispersion, which we can call a "Landau level (or subband)." However in the case of a carbon tube, the magnetic field is oscillating in the direction x with the period L, and thus there is no energy degeneracy associated with a quantum number in the direction of k_y. Further, in the 2D case, the magnetic energy levels depend on whether Ha^2/ϕ_0 is a rational or irrational number.[11] When Ha^2/ϕ_0 is rational, that is $Ha^2/\phi_0=p/q$ (p,q are integers), q Landau subbands form because of the qa translational symmetry in the direction of x for the transfer matrix element, $\propto\exp(ieHax/c\hbar)$ between y and $y+a$. The corresponding unit cell becomes of size $qa\times a$ in a magnetic field. Thus the unit cell in a magnetic field is a function of q and H, which gives a fractal spectra of Landau levels as a function of H in the case of a 2D cosine band. However, this is not the case in 1D tubes in which the total magnetic flux penetrating the surface is canceled in the front and back surface of a tube with the period L. Thus, the unit cell is always of length L in the direction of x, and the number of k_x vectors does not change by changing the magnetic field. This is the reason why we get no Landau levels over the whole energy range of the energy bandwidth. If we take the limit of $L\to\infty$, the vector potential $\mathbf{A}$ in Eq. (1) goes to $(0,Hx)$ and the number of N becomes infinite. In that case again we should consider the effect of whether $H\sqrt{3}a^2/4\phi_0$ is a rational or irrational

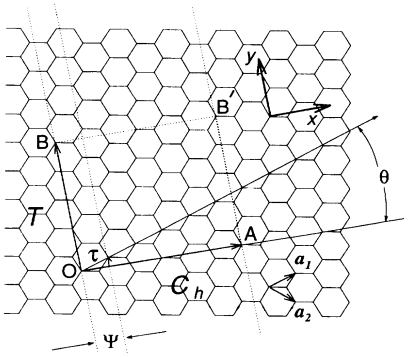

FIG. 1. Unit cell of a chiral carbon nanotube. x and y are the directions of the circumference (OA) and tube axis (OB), respectively. The figure is drawn for $\vec{C}_h=(4,2)$, $\vec{T}=(3,-5)$, $d=2$, $d_R=2$, $L=\sqrt{28}a$, $N=28$.

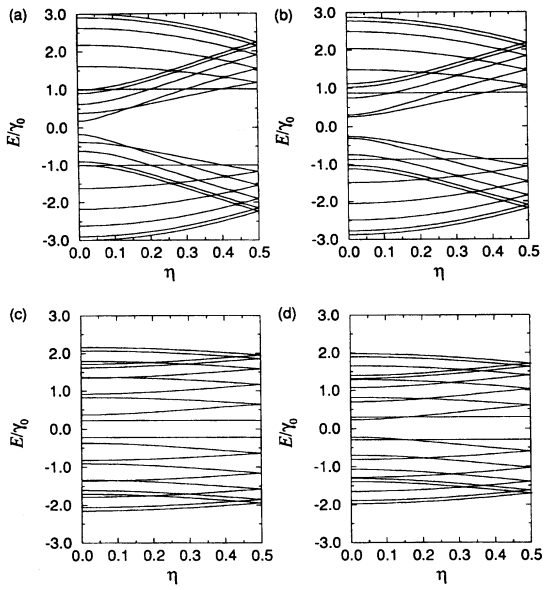

FIG. 2. Energy dispersion relations of a $\vec{C}_h=(10,0)$ carbon nanotube as a function of $\eta=k_yT/2\pi$ for several values of the dimensionless inverse magnetic length ν: (a) 0.0, (b) 1.0 (c) 2.0, (d) 3.0, where $\nu=L/2\pi\ell$ and $\ell=\sqrt{c\hbar/eH}$. The magnetic field H is perpendicular to the tubule axis.

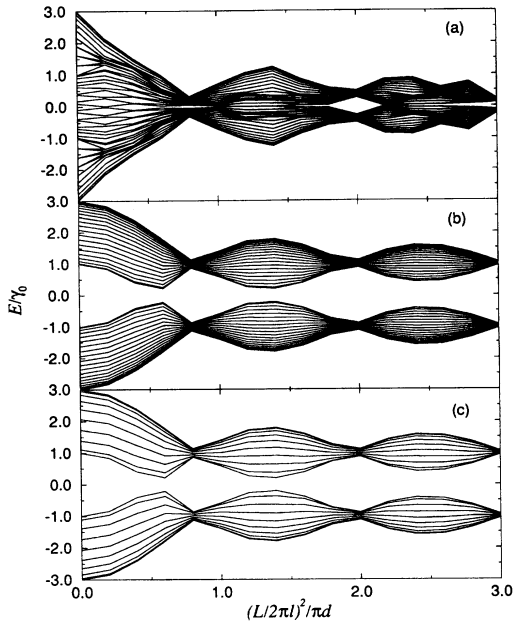

FIG. 3. The energy at $k_y=0$ as a function of a dimensionless magnetic field $(L/2\pi\ell)^2/\pi d$ for a zigzag tubule (a) $(n,m)=(20,0)$ and two armchair tubules of different diameter (n,m) = (b) (20,20) and (c) (9,9).

number, when considering two-dimensional Landau levels of graphite.[18]

When the magnetic field increases, the energy dispersion of each tubule energy band becomes narrower (see Fig. 2) because of magnetic interband interaction between different k_x bands. This narrowing is easily seen in the case of zigzag tubes for which the chiral vector $\vec{C}_h$ is expressed as $(n,0)$. For a general chiral vector, the narrowing also occurs. However, it is difficult to see this effect, since the energy dispersion curves with different symmetries can cross each other in a complicated way. This fact implies that the effective mass of the electrons increases with increasing H, and this effect might therefore be observed in a cyclotron resonance experiment. The magnetic field scale, over which the bandwidth decreases, depends on L, or the tube diameter. If the tube diameter is sufficiently large (200 Å), the phenomenon should be observable in available laboratory magnetic fields (5 T).

The total energy bandwidth decreases with increasing magnetic field (see Fig. 2) and these oscillations in bandwidth are found not to depend on k_y. The reason for the lack of k_y dependence is that k_y is a quantum number independent of H. The interband mixing effect between different k_x values is sensitive to k_y. However, when we apply higher magnetic fields, the total energy bandwidth is found to oscillate as a function of H, as shown in Fig. 3. The energy at $k_y=0$ is plotted in Fig. 3 as a function of a dimensionless magnetic field $(L/2\pi\ell)^2/\pi d$ for the three tubules $\vec{C}_h=$ (a) (20,0), (b) (20,20), and (c) (9,9). The bandwidth oscillates as a function of $(L/2\pi\ell)^2/\pi d$ for these three tubules. It is, however, stressed that the oscillations are not fully periodic, but rather the "period" and oscillation amplitude are changing with increasing magnetic field.

The main oscillation can be explained by the magnetic factor appearing in the transfer matrix elements, in which the matrix elements between k_x^p and $k_x^{p'}$ are proportional to $\sim J_{p-p'}(q)$, where $J_n(q)$ is the nth Bessel function and q is expressed as

$$q=\left(\frac{L}{2\pi\ell}\right)^2\Delta Y\,\frac{2\sin\pi\Delta X/L}{\Delta X}\equiv\left(\frac{L}{2\pi\ell}\right)^2 f(\Delta X,\Delta Y) \qquad (11)$$

in which $\Delta X,\Delta Y$ are the nearest-neighbor distances along the x and y directions. There are three possible nearest-neighbor sites which should be summed in the matrix elements. From Eq. (11), the energy dispersion is a function of the product of the dimensionless magnetic field $(L/2\pi\ell)^2$ and a factor $f(\Delta X,\Delta Y)$ which is related to the symmetry of the tube. In the case of Fig. 3, the curves show that for the high symmetry zigzag tubes $(n,0)$ and armchair tubes (n,n), the energy dispersion relations may be scaled by $J_0[(L/2\pi\ell)^2c/d]$ (where c is constant). For more general (n,m) chiral fibers, we can see the same shape of oscillation as in Fig. 3. However, in the general case, the scaling factor depends on the tubule symmetry and the scaling factor is not always equal to d, the highest common denominator of (n,m).

It is interesting to see for a semiconducting tube (20,0) that the energy gap at the Fermi energy $E_F=0$ is oscillating between the zero-field band-gap value and 0 as a function of magnetic field. This means that the semiconducting tube can be either metallic or semiconducting with increasing magnetic field, dependent on the H values. This phenomenon was already pointed out in the case that the magnetic field is parallel to the fiber axis.[13] This result, however, is not found in the $\vec{k}\cdot\vec{p}$ perturbation theory calculation when the magnetic field is perpendicular to the tube axis. The oscillations in Fig. 3 can be found only when we consider the symmetry effect of the carbon nanotube, which gives rise to a finite number of wave vectors in the k_x direction. This phenomenon can be

seen also for metallic tubes if we select only those k_y values which cross the K points. It is noted here that all k_x values with a fixed k_y are mixed with each other. If a given k_y value does not cross the K point, it is generally impossible to achieve the $E=0$ condition with any mixing of k_x values.

It is important to note here that we neglected the Zeeman term ($Hg\sigma\mu_B$) in the present calculation for simplicity. Lin-Chung and Rajagopal pointed out that the oscillation of the magnetic moment as a function of magnetic field (Aharanov-Bohm effect) is significantly affected by this spin-paramagnetic contribution when the magnetic field is along the tubule axis.[19] The Zeeman effect should also be taken into account in the present calculation when the magnetic field is perpendicular to the tubule axis. When the interaction for the hopping matrix element is spin independent, as in our simple tight-binding calculation, each magnetic energy band is split into spin-up and spin-down bands by $\pm H\mu_B$, where we assume $g=2$ and $\sigma=1/2$. Here the direction of the spin is defined along the direction of the magnetic field and we imagine that an electron transfers from one atomic site to another without changing spin direction. If the Zeeman splitting of the energy bands is larger than the energy gap near the Fermi energy, then the electron and hole Fermi surfaces form in the Zeeman-split energy bands. Such large magnetic fields could make a semiconducting tubule become semimetallic. Since the energy gap of a semiconducting tubule does not depend on tubule chirality, but is inversely proportional to the tubule diameter,[15] we can estimate the magnetic field corresponding to an energy gap $E_g=2\mu_B H$ (for $E_g=0.275$ eV and $d_t=100$ Å), obtaining $H\sim 2300$ T. Thus the small oscillation of the energy gap observed in the semiconducting (20,0) tubule may still be observed when we include the Zeeman term. As for the case of metallic tubules, the Zeeman term would affect the magnetic susceptibility, as discussed by Lin-Chung and Rajagopal.[19] The competition between the Zeeman term and the lattice geometry (or lattice potential) is not simple for the larger diameter tubules and higher magnetic fields, and a more detailed treatment of this effect will be reported elsewhere.

In the case of the armchair nanotubes (20,20) and (9,9) the energy levels in the first period of the magnetic field are identical to the energy dispersion for these tubes in the direction of k_y in the case of $H=0$. In such a high symmetry case, we can see that application of a weak field corresponds to a shift of the k_y vector in the T direction (see Fig. 1). It is not easy to see this relation for a general chiral tube.

Such large oscillations might be observed in carbon nanotubes with very large diameters, since the period is basically proportional to the inverse of the square of the diameter (in the case of Fig. 3, the period is proportional to the inverse of the diameter, since da is the order of L). For example, in the case of a (74,74) tube whose diameter is 100.4 Å, the first node of the oscillation corresponds to 470 T, which is still a very large field value for an experiment. However this is the worst case, since the tube with a large d has the highest symmetry. If we take the lowest symmetry case with $d=1$ and with a tubule diameter d_t in Å, and we assume that the symmetry factor $f(\Delta X,\Delta Y)$ is ~ 1, the first mode occurs at a field of $2\times 10^4/d_t^2$ T which is only 2 T for a d_t value of ~ 100 Å.

As seen above, for a given diameter d_t, the symmetry factor $f(\Delta X,\Delta Y)$ in Eq. (11) is essential for determining the period, since we can see that the tubules (20,0) and (20,20), whose diameters differ by a factor of $\sqrt{3}$, have the same period. Further, the difference between the highest symmetry case and the lowest symmetry case are on the order of 2 for $d_t=100$ Å. Thus, the observation of this oscillation may provide a tool for determining the chirality of a carbon nanotube. Furthermore, the oscillation of the total energy of the π bands could give rise to a large oscillation in the magnetic susceptibility. It is noted that these oscillations are different from the usual de Haas–van Alphen oscillations, where the period of oscillation is proportional to H. Furthermore, the oscillations in the density of states and in the effective mass of the 1D carbon nanotubes at the Fermi level would give rise to interesting phenomena in the magnetoresistance at very low temperature. In the experiments, the effect of multilayers would tend to cancel the oscillation from tubules of different diameters and symmetries. A large diameter single-wall carbon nanotube would therefore be preferable for experimental study. A more detailed report on the properties of the magnetic energy band structure for carbon nanotubes will be presented elsewhere.

The research at MIT was funded by NSF Grant No. DMR-92-01878. One of the authors (R.S.) acknowledges the Japan Society for the Promotion of Science for supporting his visit to MIT by the US-Japan cooperative research program, and the MIT authors (G.D. and M.S.D.) acknowledge corresponding support by NSF Grant No. INT 94-90144 from the U.S.-Japan program. Part of the work by R.S. was supported by a Grant-in-Aid for Scientific Research in Priority Area "Carbon Cluster" (Area No. 234/05233214) from the Ministry of Education, Science and Culture, Japan.

[1] S. Iijima, Nature (London) **354**, 56 (1991).
[2] M. S. Dresselhaus *et al.*, Phys. Rev. B **45**, 6234 (1992).
[3] J. W. Mintmire *et al.*, Phys. Rev. Lett. **68**, 631 (1992).
[4] R. Saito *et al.*, Phys. Rev. B **46**, 1804 (1992).
[5] R. Saito *et al.*, Appl. Phys. Lett. **60**, 2204 (1992).
[6] N. Hamada *et al.*, Phys. Rev. Lett. **68**, 1579 (1992).
[7] K. Tanaka *et al.*, Chem. Phys. Lett. **191**, 469 (1992).
[8] L. Langer *et al.*, J. Mater. Res. **9**, 927 (1994).
[9] J. Heremans *et al.*, Phys. Rev. B **49**, 15 122 (1994).
[10] X. K. Wang *et al.*, J. Mater. Res. **9**, 1578 (1994).
[11] D. R. Hofstadter, Phys. Rev. B **14**, 2239 (1976).
[12] F. A. Butler and E. Brown, Phys. Rev. **166**, 630 (1968).
[13] H. Ajiki and T. Ando, J. Phys. Soc. Jpn. **62**, 1255 (1993); **62**, 2470 (1993).
[14] R. A. Jishi *et al.*, Phys. Rev. B **47**, 16 671 (1993).
[15] R. A. Jishi *et al.*, J. Phys. Soc. Jpn. **63**, 2252 (1994).
[16] J. M. Luttinger, Phys. Rev. **84**, 814 (1951).
[17] R. Saito *et al.*, Phys. Rev. B **50**, 5680 (1994).
[18] J. W. McClure, Phys. Rev. **104**, 666 (1956).
[19] P. J. Lin-Chung and A. K. Rajagopal, Phys. Rev. B **49**, 8454 (1994).

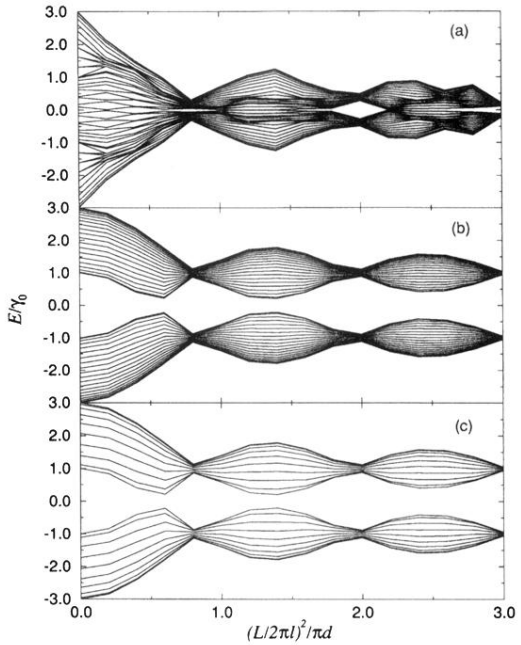

FIG. 3. The energy at $k_y=0$ as a function of a dimensionless magnetic field $(L/2\pi\ell)^2/\pi d$ for a zigzag tubule (a) (n,m) $=(20,0)$ and two armchair tubules of different diameter (n,m) = (b) (20,20) and (c) (9,9).